SIMULATION OF THE UPWARD GOING FLUX OF THERMAL RADIATION SCATTERED BY AEROSOL

PART III. VOLCANIC STRATOSPHERIC AEROSOL

S.V. Afonin, V.V. Belov, and I.Yu. Makushkina

Institute of Atmospheric Optics,
Siberian Branch of the Russian Academy of Sciences, Tomsk
Received March 10, 1994

We consider some results of simulation of the upward going flux of thermal radiation of the "atmosphere−underlying surface" system for various contents of volcanic stratospheric aerosol. The effect of aerosol on the intensity, structure, and spatial characteristics of the flux of thermal radiation is studied in a wide range of optical and geometric situations using the Monte Carlo method and several approximate techniques.

1. INTRODUCTION

Earlier[1,2] we presented some results of the studies of the intensity, structure, and spatial characteristics of the upward going flux of thermal radiation of the atmosphere and the underlying surface scattered by aerosol in spectral ranges of 3.5−4.0 and 10.3−11.3 μm. These results referred to the case of wide variations of the optical parameters of aerosol in the boundary atmospheric layer for background tropospheric and stratospheric contents of aerosol.

However, it is well known that volcanic activity may yield aerosol layers with "abnormal" optical characteristics, different from the background situation in the stratosphere. According to the authors of Ref. 3, the occurrence of such layers may noticeably affect the accuracy of satellite measurements of the surface temperature. Despite the attempts to modify the available operative algorithms for atmospheric correction of satellite data, so as to apply them to such situations,[3] one still needs for a comprehensive and accurate way to account for aerosol produced perturbations of data of remote sensing of the underlying surface. Such an approach calls for additional studies of the formation and characteristics of the upward going flux of thermal radiation scattered by aerosol in a post−volcanic situation.

In what is to follow, we consider the effect of volcanic stratospheric aerosol on the intensity, structure, and spatial characteristics of the flux of scattered thermal radiation over a spatially homogeneous Lambertian surface. Besides, we estimate the accuracy of the approximate models for single and "conservative" scattering of radiation.

2. BASIC CHARACTERISTICS OF SIMULATION

In our simulation we aimed at obtaining the following characteristics:

a) The radiance J_λ and radiative temperature T_λ of free radiation of the "atmosphere−underlying surface" (A−US) system

$$J_\lambda = J_\lambda^0 + J_\lambda^{MS} , \quad J_\lambda^{MS} = J_{atm}^{MS} + J_{surf}^{MS} ,$$

$$T_\lambda^{MS} = B_\lambda^{-1} [J_\lambda] , \quad T_\lambda^0 = B_\lambda^{-1} [J_\lambda^0] ,$$

where J_λ^0 and T_λ^0 are the characteristics of non−scattered radiation; J_λ^{MS} is the intensity of scattered radiation; J_{surf}^{MS} is the contribution to J_λ^{MS} from the underlying surface; J_{atm}^{MS} is the contribution to J_λ^{MS} from the atmosphere.

All these variables are wavelength dependent, therefore we omit the "λ" index for brevity reasons.

The simulation was carried out accounting for multiple scattering (MS model), single scattering (SS model), and conservative scattering (CS model).

Temperature corrections were computed along with the intensity of scattered radiation:

$$\Delta T_\lambda^{MS} = T_\lambda^{MS} - T_\lambda^0 , \quad \Delta T_\lambda^{SS} = T_\lambda^{SS} - T_\lambda^0 ,$$

as well as the values ΔT_{atm}^{MS} and ΔT_{atm}^{SS} which reflect the contribution from the atmosphere to the intensity of scattered radiation.

To estimate the effect of aerosol on the radiative temperature we calculated:

$$d T_{aer} = T_\lambda^{mol} - T_\lambda^{MS} ,$$

where T_λ^{mol} is the radiative temperature of the A−US system in the case of a purely molecular atmosphere.

To estimate the accuracy of the approximate models of single and conservative scattering we calculated the values:

$$d T_{CS} = T_\lambda^{MS} - T_\lambda^{CS} , \qquad d T_{SS} = T_\lambda^{MS} - T_\lambda^{SS} ,$$

and also $d T_{SS}$ (atm).

Additional calculations showed that the combined effect of aerosol present in the boundary layer and the stratosphere on the radiative temperature of the A−US system may, with the account for the error level of approximate models, be estimated to a high degree of accuracy (better than 0.5−1.0°) by a direct arithmetic summation of ΔT_λ^{MS}, $d T_{CS}$, $d T_{SS}$, $d T_{aer}$ taken separately

for the boundary aerosol (Ref. 1), and the stratospheric aerosol (see the present study).

b) Spatial distribution of the intensity of lateral illumination $J_{\text{surf}}^{\text{MS}}(R)$.

c) Contribution from a unit surface areas, remoted to distance r from the point of sighting, to the intensity of scattered radiation (if being normalized by $J_{\text{surf}}^{\text{MS}}$, then the relative contribution):

$$F(r) = \frac{1}{2\pi r} \frac{\partial J_{\text{surf}}^{\text{MS}}(r)}{\partial r} .$$

d) The radius of lateral illumination, found from the condition

$$T_\lambda - T_\lambda(R) = \delta T_\lambda ,$$

where δT_λ is a preset level of computational accuracy for the radiative temperature T_λ, from the range $0.1° < \delta T_\lambda < 1°$.

A more detailed definition of the variables listed above together with the description of algorithms used to compute them according to various models, may be found in Refs. 1 and 2.

3. OPTICAL AND GEOMETRIC CONDITIONS USED IN SIMULATION

The optical and geometric configurations chosen to simulate observations are as follows: spectral ranges of 3.55–3.95 μm ($\lambda = 3.75$ μm) and 10.3–11.3 μm ($\lambda = 10.8$ μm), angles of observation: $\varphi = 0$ and 45°, observation altitude of 800 km. The atmosphere was assumed spherically symmetric and vertically stratified. Meteorological models of the atmosphere included the tropics, midlaltitudinal summer and winter, the arctic summer, and standard US–1976 model. Aerosol models covered moderate, high, and extreme content of volcanic aerosol in the stratosphere, while the boundary layer was assumed free of aerosol. The underlying surface was assumed spatially homogeneous, Lambertian, and emitting as a black body within the temperature range 272.2–299.7 K.

Vertical profiles of meteorological parameters of the atmosphere, the coefficients of molecular and aerosol extinction (scattering) were obtained from the data compiled in the LOWTRAN–7 code.[4]

Figure 1 presents typical profiles of coefficients of aerosol extinction for various types of volcanic aerosol, as compared to its background content in the stratosphere, and the angular dependence of scattering phase function. Table I lists the range of seasonal variability of aerosol optical depth τ_{sct} and of the aerosol scattering to extinction ratio.

TABLE I. Ranges of optical thickness of aerosol (due to scattering) τ_{sct} and of scattering to extinction ratio.

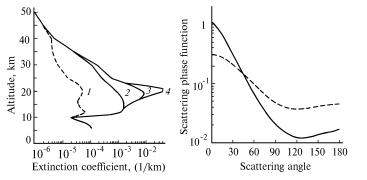| Aerosol content	$\lambda = 3.75$ μm		$\lambda = 10.8$ μm	
	τ_{sct}	ratio	τ_{sct}	ratio
Moderate	0.0150	0.9434	0.0048	0.4752
	0.0145	0.9477	0.0047	0.4896
High	0.0501	0.9471	0.0164	0.4940
	0.0397	0.9475	0.0130	0.4962
Extreme	0.1385	0.9480	0.455	0.4978
	0.1353	0.9481	0.0445	0.4989

Fig.1. Vertical profile of coefficients of aerosol extinction for various contents of stratospheric volcanic aerosol: background (1), moderate (2), high (3), and extreme (4).
Angular dependence of the scattering phase function: $\lambda = 3.75$ μm (solid line), $\lambda = 10.8$ μm (dashed line).

4. SIMULATION RESULTS

Some results of simulation are presented in Figs. 2, 3 and in Tables II–IV.

Table II lists the data on the effect of aerosol (dT_{aer}) on the radiative temperature and estimated accuracy level resulting from the models of single and conservative scattering (dT_{SS}, $dT_{\text{SS}}(\text{atm})$, dT_{CS}).

Table III contains the maximum temperature corrections DT_λ^{MS} and $DT_{\text{atm}}^{\text{MS}}$ and the range of their seasonal variations for various optical and geometric conditions of observations.

Table IV lists the maximum radii R for various contents of volcanic stratospheric aerosol and the range of R variability due to variations of meteorological parameters of the atmosphere.

Fig. 2 illustrates the dependence of the radius of lateral illumination on the computational accuracy assumed for radiative temperature.
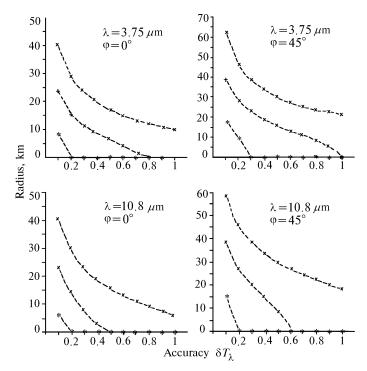
Fig. 2. Radius of lateral illumination vs. computational accuracy of radiative temperature for various contents of stratospheric volcanic aerosol (midlatitudinal summer): extreme (x), high (+), and moderate (∗).

TABLE II. Computational errors for radiative temperature when using models of single and conservative scattering for moderate, high, and extreme contents of volcanic aerosol.

Aerosol content	$\varphi = 0°$				$\varphi = 45°$			
	mol–MS	MS–CS	MS–SS Total	MS–SS Atmosphere	mol–MS	MS–CS	MS–SS Total	MS–SS Atmosphere
	$\lambda = 3.75$ μm							
Moderate	0.093	0.275	0.005	0.001	0.161	0.419	0.010	0.003
High	0.246	0.953	0.032	0.010	0.529	1.409	0.080	0.030
Extreme	0.681	2.610	0.210	0.065	1.389	3.904	0.489	0.171
	$\lambda = 10.8$ μm							
Moderate	0.330	0.203	0.002	0.002	0.603	0.251	0.004	0.002
High	1.220	0.602	0.016	0.009	2.015	0.902	0.035	0.024
Extreme	3.307	1.650	0.096	0.064	5.490	2.372	0.192	0.133

TABLE III. Maximum temperature corrections ΔT_l^{MS} and ΔT_{atm}^{MS} (K) and their maximum seasonal variations for volcanic stratospheric aerosol.

Aerosol content		$\varphi = 0°$		$\varphi = 45°$	
		Total	Atmosphere	Total	Atmosphere
		$\lambda = 3.75$ μm			
Moderate	maximum value	0.300	0.065	0.358	0.132
	maximum variations	0.050	0.034	0.029	0.067
High	maximum value	0.944	0.237	0.423	0.501
	maximum variations	0.260	0.150	0.535	0.320
Extreme	maximum value	2.640	0.646	3.936	1.283
	maximum variations	0.346	0.400	0.562	0.734
		$\lambda = 10.8$ μm			
Moderate	maximum value	0.257	0.137	0.368	0.266
	maximum variations	0.088	0.098	0.063	0.190
High	maximum value	0.764	0.434	1.120	0.719
	maximum variations	0.253	0.308	0.225	0.442
Extreme	maximum value	2.088	1.202	3.077	1.977
	maximum variations	0.225	0.765	0.212	1.148

TABLE IV. *Maximum radii of lateral illumination* (km) *and maximum ranges of their seasonal variations for multiple scattering.*

Aerosol content		$\varphi = 0°$			$\varphi = 45°$		
		Accuracy ($\delta\,T_\lambda$)			Accuracy ($\delta\,T_\lambda$)		
		1	0.5	0.1	1	0.5	0.1
$\lambda = 3.75\ \mu m$							
Moderate	maximum value			11.721			21.326
	maximum variations			4.160			3.215
High	maximum value		6.714	23.999	6.214	17.735	44.709
	maximum variations		3.978	5.337	6.214	5.262	8.384
Extreme	maximum value	11.079	19.185	46.923	23.852	34.759	76.034
	maximum variations	2.020	2.813	8.973	3.535	5.643	19.193
$\lambda = 10.8\ \mu m$							
Moderate	maximum value			14.626			25.514
	maximum variations			9.083			14.189
High	maximum value		4.648	34.039		18.196	52.744
	maximum variations		4.648	16.598		18.196	21.721
Extreme	maximum value	11.367	23.173	59.897	25.790	39.587	87.859
	maximum variations	11.367	11.618	28.281	17.061	15.498	41.359

Fig. 3 plots the $F(r)$ function for the case of extreme aerosol content in the stratosphere.

Analysis of simulation results makes it possible to identify the following features in the process of formation of the upward going flux of thermal radiation, scattered by the layer of stratospheric aerosol.

1. To reach a computational accuracy of 0.5–1° in radiative temperature, one needs to account for the perturbing effect of stratospheric aerosol in the case when the optical thickness of aerosol (due to scattering) exceeds $\tau_{sct} > 0.090$ at $\lambda = 3.75\ \mu m$ (high aerosol content) and $\tau_{sct} > 0.007$ at $\lambda = 10.8\ \mu m$ (moderate aerosol content, see Table II).

2. In contrast to the case of boundary layer aerosol, when the contribution from the underlying surface (J_{surf}^{MS})
to intensity of scattered thermal radiation dominates,[1] there can occur such situations with the stratospheric aerosol when the atmospheric contribution (J_{atm}^{MS}) may be either comparable to or even exceed J_{surf}^{MS} reaching 1–2° in terms of temperature corrections (these situations would be encountered at high atmospheric temperatures and moisture content, see Table III).

3. The dependence of temperature corrections on the optical thickness of atmospheric aerosol may be approximated by a linear function to a high degree of accuracy (better than 0.1°).

4. When simulating the process of transfer of thermal radiation in the presence of stratospheric aerosol, it is sufficient to use the single scattering approximation. Simulation error remains below 0.5° (see Table II).
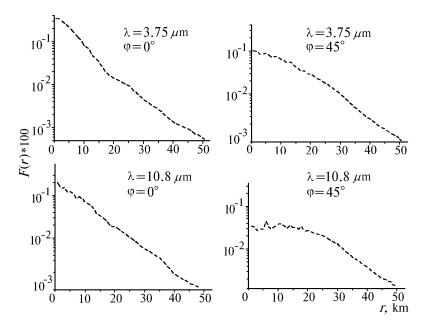

Fig. 3 *Relative contribution from surface elements* $F(r)$ *into the intensity of lateral illumination vs. range from the point of sighting for extreme content of stratospheric volcanic aerosol* (*midlatitudinal summer*).

5. Despite the wide variability of meteorological parameters of the atmosphere and of the underlying surface temperature, seasonal variations of $D T_\lambda^{MS}$ do not exceed 0.6° at $\lambda = 3.75$ μm and 0.3° at $\lambda = 10.8$ μm (see Table III). Thus, approximating $D T_\lambda^{MS}$ by its average for the considered season does not result in a decrease computational accuracy for the radiative temperature below 0.5−1.0°.

6. Comparing the approximate models of single and conservative scattering, which account for the distorting effect of aerosol, one obtains that the model of single scattering offers a much lower error level within the covered range of optical and geometric conditions (better than 0.5°). It is not recommended to apply the model of conservative scattering then, since the error it yields at $\lambda = 3.75$ μm exceeds the level of aerosol effect itself $d T_{aer}$ and does not provide for the necessary accuracy of 0.5−1.0° at $\lambda = 10.8$ μm (see Table II).

The analysis of spatial characteristics of lateral illumination yields features both similar to the case of the boundary layer aerosol, and typical exclusively for stratospheric volcanic aerosol.

1. A dependence of the radius of lateral illumination on the computational accuracy of radiative temperature for stratospheric aerosol is identical to that for aerosol in the boundary layer, namely, for higher accuracies δT_λ the radius R of lateral illumination monotonouslically increases (Fig. 2). Note that R grows much faster in the range $\delta T_\lambda = 0.5-1.0°$ (increasing by up to a factor of eight), as compared to the range of $1.0 - 0.5°$ (the factor is only of $1.5 - 3.0°$), see Fig. 2 and Table IV.

2. An increase of the optical thickness of aerosol (due to scattering) results in a monotonic growth of the radius of lateral illumination, which reaches the following values in case of extremely high content of volcanic aerosol (see Table IV):

for $\delta T_\lambda = 1.0°$: $R = 10-25$ km ($\lambda = 3.75$ μm), and $R = 10-25$ km ($\lambda = 10.8$ μm), for $\delta T_\lambda = 0.5°$: $R = 20-35$ km ($\lambda = 3.75$ μm), and $R = 25-40$ km ($\lambda = 10.8$ μm).

3. The contribution from surface elements to the intensity of lateral illumination monotonically decreases as one moves away from the sighting point, as illustrated by the dependence $F(r)$ in Fig. 3. However, in the case of volcanic aerosol the behavior of $F(r)$ becomes much smoother, so that $F(r)$ drops by a factor of 10 at distances of 15−40 km, compare that with the case of the boundary layer aerosol when the principal contribution (more than 60%) belongs to the surface area of radius $R = 1$ km, while the $F(r)$ function drops by a factor of 15−20 within the range $r = 1-2$ km.

Summarizing the above said we formulate the main conclusions of this study as follows:

1. When simulating the process of transfer of thermal radiation through stratospheric aerosol one may neglect the effects of multiple scattering. Employing the single−scattering approximation, a computational accuracy better than 0.5° can be achieved for radiative temperature. At the same time the approximate model of conservative scattering does not necessarily provide the desired accuracy at high content of stratospheric aerosol. To reach a computational accuracy of at least 0.5−1.0° in radiative temperature the lateral illumination area of at least 10 (10−40) km radius should be considered. If higher accuracy required ($\simeq 1.0°$), the radius of lateral illumination increases to 25−90 km.

2. In practice the contribution from stratospheric aerosol into the flux of upward going thermal radiation may, to a high degree of accuracy, be computed using linear approximation of the dependence of temperature corrections on the optical thickness of aerosol.

3. If the accuracy of 0.5−1.0° required for remote sensing of the underlying surface temperature, the effective size of the area forming lateral illumination under high content of stratospheric aerosol significantly exceeds the linear size of the instant field of view of satellite systems, which are used for remote sensing of the underlying surface at middle and high spatial resolution (which is below 0.5−1.0 km). This fact should be taken into account when interpreting results of remote sensing of underlying surface being characterized by noticeable temperature inhomogeneities outside the field of view of a sensing system.

REFERENCES

1. S.V. Afonin, V.V. Belov, and I.Yu. Makushkina, ibid., Part I, Atmos Oceanic Opt. **7**, No. 6, 423-429 (1994).
2. S.V. Afonin, V.V. Belov, and I.Yu. Makushkina, Atmos Oceanic Opt. **7**, No. 6, 430-434 (1994).
3. R. Richter, Int. J. Remote Sensing **6**, No. 11, 1773−1777 (1985).
4. F.X. Kneizys et al., "User's Guide to LOWTRAN−7", AFGL−TR−88−0177, ERP, No. 1010, AFGL, Hansom AFB, MA 01731.